Seasonal Locking of the MJO's Southward Detour of the Maritime Continent: The Role of the Australian Monsoon

DAEHYUN KANG,^a DAEHYUN KIM^o,^b STEPHANIE RUSHLEY,^c AND ERIC MALONEY^d

^a Center for Sustainable Environment Research, Korea Institute of Science and Technology, Seoul, South Korea
 ^b Department of Atmospheric Sciences, University of Washington, Seattle, Washington
 ^c National Research Council, Naval Research Laboratory, Monterey, California
 ^d Department of Atmospheric Science, Colorado State University, Fort Collins, Colorado

(Manuscript received 10 April 2022, in final form 13 August 2022)

ABSTRACT: This study investigates why the major convective envelope of the Madden–Julian oscillation (MJO) detours to the south of the Maritime Continent (MC) only during boreal winter [December–March (DJFM)]. To examine processes affecting this MJO detour, the MJO-related variance of precipitation and column-integrated moisture anomalies in DJFM are compared with those in the seasons before [October–November (ON)] and after [April–May (AM)]. While MJO precipitation variance is much higher in the southern MC (SMC) during DJFM than in other seasons, the MJO moisture variance is comparable among the seasons, implying that the seasonal locking of the MJO's southward detour cannot be explained by the magnitude of moisture anomalies alone. The higher precipitation variance in the SMC region is partly explained by the much higher moisture sensitivity of precipitation in DJFM than in other seasons, resulting in a more efficient conversion of anomalous moisture to anomalous precipitation. DJFM is also distinguishable from the other seasons by stronger positive wind–evaporation feedback onto MJO precipitation anomalies due to the background westerly wind in the lower troposphere. It is found that the seasonal cycle of moisture–precipitation coupling and wind–evaporation feedback in the SMC region closely follows that of the Australian monsoon, which is active exclusively in DJFM. Our results suggest that the MJO's southward detour in the MC is seasonally locked because it occurs preferentially when the Australian monsoon system produces a background state that is favorable for MJO development in the SMC.

KEYWORDS: Maritime Continent; Madden-Julian oscillation; Monsoons; Moisture/moisture budget; Intraseasonal variability; Seasonal cycle

1. Introduction

The Madden-Julian oscillation (MJO; Madden and Julian 1971, 1972) is the dominant mode of tropical intraseasonal variability. Associated with the MJO, anomalously enhanced or suppressed convection coupled with planetary-scale circulation anomalies propagates eastward at a speed of about 5 m s⁻¹ over the Indo-Pacific warm pool. The MJO affects many types of tropical weather and climate phenomena, such as the formation of tropical cyclones (Liebmann et al. 1994; Maloney and Hartmann 2000), the Indian and Australian monsoons (Yasunari 1979; Wheeler and McBride 2005), and El Niño development (Takayabu et al. 1999; Kessler 2001). Moreover, the anomalous diabatic heating associated with the MJO influences circulations in the mid- to high latitudes through Rossby wave propagation (Matthews et al. 2004; Lin et al. 2009; Lee and Lim 2012; Seo and Son 2012; Dole et al. 2014; Adames and Wallace 2014; Tseng et al. 2019). With profound impacts on atmospheric circulations worldwide, the MJO provides a primary source of subseasonal predictability in the global climate system (Kim et al. 2018; Meehl et al. 2021).

Oenotes content that is immediately available upon publication as open access.

Corresponding author: Daehyun Kim, daehyun@uw.edu

Despite the progress made in the past decades on understanding the MJO, the answers to many fundamental questions about its observed characteristics remain incomplete. One such aspect is the MJO's characteristics in the Maritime Continent (MC) region, where the MJO exhibits peculiar behavior that are not present in the other areas [see Kim et al. (2020) and Jiang et al. (2020) for reviews on this topic]. The eastwardpropagating MJO convective envelope that develops in the eastern Indian Ocean often weakens or ceases when it encounters the MC. This so-called "MC barrier effect" (Kim et al. 2014; Zhang and Ling 2017; Kerns and Chen 2016) is exaggerated in global climate models (GCMs), in which the MJO tends to be interrupted in the MC region more frequently than observed (Jiang et al. 2015; Ling et al. 2017; Ahn et al. 2020a). Also, unlike in the Indian Ocean where the MJO's main convective activity occurs near the equator, in the vicinity of the MC the majority of MJO convection tends to propagate in the summer hemisphere (Knutson et al. 1986; Wang and Rui 1990; Zhang and Ling 2017), or in other words, the MJO "detours" the MC (Wu and Hsu 2009; Kim et al. 2017). Partly due to the limited understanding of the processes responsible for the MJO's peculiar behavior over the MC, many contemporary climate models fail to simulate realistic MJO activity across the MC region (Jiang et al. 2015; Ahn et al. 2020b).

Many efforts have been made to understand the mechanisms behind the MJO's peculiar behavior in the MC (e.g., Wu and Hsu 2009; Sobel et al. 2010; Kim et al. 2017; Zhou

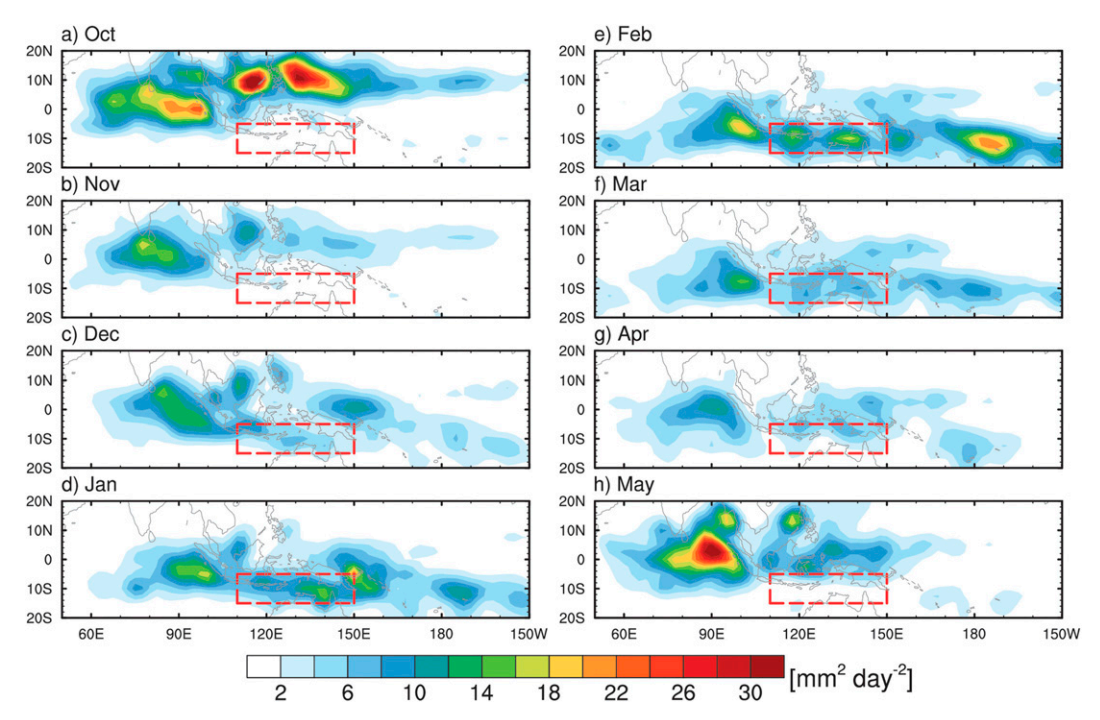


Fig. 1. Variance of daily MJO precipitation anomalies (mm² day⁻²) in each month from October to May for 1998–2018.

The red boxes indicate the SMC region.

and Murtugudde 2020). Wu and Hsu (2009) suggested a crucial role for MC topography in the development of the major MJO convective envelop south of the equatorial islands during boreal winter. Sobel et al. (2008, 2010) suggested that intraseasonal variability of convection is preferred over the ocean because surface latent heat flux is limited in the MC islands near the equator, explaining why MJO variability weakens there. Kim et al. (2017) proposed a "differential moistening hypothesis" that attributes the southward detour in boreal winter as a consequence of the greater moisture supply by horizontal advection in the southern MC (SMC) than near the equator (Kim et al. 2017). Meanwhile, Zhou and Murtugudde (2020) found that warm sea surface temperature (SST) anomalies in the SMC appear before the onset of the MJO and suggested their role in the development of MJOassociated convective anomalies.

Another group of studies has attempted to address the question of why the southward detour of the MJO occurs only in boreal winter (Zhang and Dong 2004; Kim et al. 2017; Singh and Kinter 2020). For example, Zhang and Dong (2004) and Singh and Kinter (2020) showed that the seasonal cycle of the MJO variability covaries with that of mean-state variables such as SST, zonal wind, column moisture, and lower-tropospheric moisture convergence. They found that the MJO variability was stronger in the region with favorable seasonal conditions for deep convection including warm SST, low-level westerly winds, a moist atmosphere, and stronger moisture convergence, although the seasonal cycle of SST was less strongly related with that of the MJO variability than the other variables (Zhang and

Dong 2004). Meanwhile, Kim et al. (2017) suggested that the larger zonal moisture advection, which is crucial to the southward detour, is a consequence of the higher mean zonal moisture gradient in the SMC than the equatorial MC. While these studies have presented some strong hypotheses, no consensus exists on the specific mean-state variables that are key to the seasonal locking.

This study aims to investigate processes responsible for the seasonal locking of the MJO MC detour during December–March (DJFM). We will first assess monthly MJO activity and the mean state in boreal winter (DJFM) and the seasons before [October–November (ON)] and after [April–May (AM)]. We will then examine the influence of the mean-state differences in moisture–precipitation coupling (Bretherton et al. 2004; Rushley et al. 2018; Adames 2017) and wind–evaporation feedback (Maloney and Sobel 2004; Sobel et al. 2010) that have been hypothesized to be important for MJO convective development. Then, the seasonal cycle of the MJO activity will be assessed relative to the mean-state variables.

This manuscript is organized as follows. Section 2 describes the data and methodology employed in our study. In section 3, we examine the processes responsible for the southward detour of the MJO and investigate the role of the mean state. Section 4 presents a summary and conclusions.

2. Data and method

a. Dataset

We use daily averaged precipitation from the Tropical Rainfall Measuring Mission 3B42, version 7, product (TRMM 3B42v7; Huffman et al. 2007). Atmospheric state variables are obtained from the fifth generation of the European Centre for Medium-Range Weather Forecasts (ECMWF) reanalysis (ERA5) product (Hersbach et al. 2019). A gridded SST product from the Hadley Centre Sea Ice and Sea Surface Temperature (HadISST; Rayner 2003) is used to examine the spatial distribution of SST. The datasets are obtained for the period 1998–2018 and interpolated onto a $2.5^{\circ} \times 2.5^{\circ}$ horizontal grid.

b. Methods

Most of the analysis performed in this study is done with MJO anomalies. We define MJO anomalies as those that can be reconstructed from the Real-Time Multivariate MJO (RMM) index of Wheeler and Hendon (2004). Specifically, we first calculate the daily anomalies of each variable by removing the mean and first three harmonics of the climatological seasonal cycle. Then we obtain two maps of regression coefficients by regressing daily anomalies onto RMM1 and RMM2. To account for the MJO's seasonality, the regression maps are obtained separately for each calendar day using a 31-day moving window centered on the day of interest. The MJO anomalies for a given day are then obtained by multiplying RMM1 and RMM2 on that day by their corresponding regression maps and adding the two products. Despite the caveat that the resulting MJO anomaly does not perfectly explain the entire MJO variability, it represents a significant portion of MJO characteristics in the vicinity of MC including both zonal and meridional variation. The MJO life cycle composite analysis (Wheeler and Hendon 2004) is performed by averaging a variable of interest for each phase of the MJO over days with MJO amplitude stronger than 1, as defined by the RMM index.

3. Results

a. Seasonality of the MJO and the mean state in the SMC

Figure 1 displays the variance of MJO precipitation anomalies in each month from October to May. The monthly MJO precipitation variance exhibits a prominent seasonal cycle in the vicinity of the MC. In October (Fig. 1a), precipitation variance peaks to the north of the equator. The zonally elongated envelope of high precipitation variance migrates southward into the Southern Hemisphere in the following months, reaching its greatest southern extent in February, and then moves back to the north. Consistent with the result of Zhang and Dong (2004), the meridional migration of the maximum precipitation variance is less prominent in the Indian Ocean than in the MC and the equatorial western Pacific. Instead, in the equatorial Indian Ocean, the seasonal cycle of MJO precipitation variance is mostly related to the magnitude, with relatively lower variance in boreal winter months than in May and October.

Focusing on the SMC region (red box in Fig. 1), notable MJO variability appears only from December to March, with

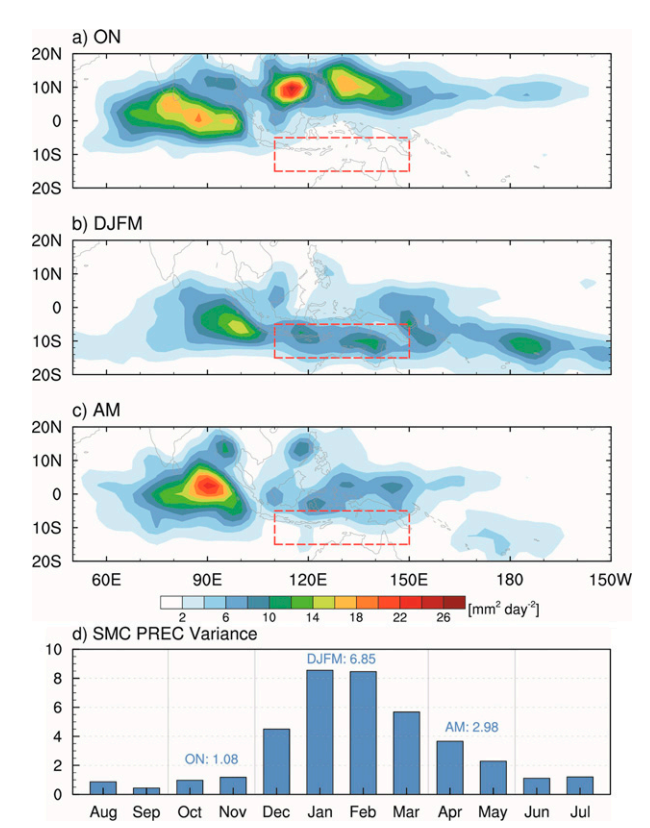


FIG. 2. As in Fig. 1, but for the variance during (a) ON, (b) DJFM, and (c) AM. (d) Climatological seasonal cycle of area-averaged MJO precipitation variance (mm² day⁻²) in the SMC region. In (d), the numbers over the bar graphs indicate the variance calculated in ON, DJFM, and AM (from left to right). The red boxes indicate the SMC region.

much weaker variance in the months before (ON) and after (AM). This seasonality of MJO variance is more clearly shown in Fig. 2. Unlike the southward MJO detour in DJFM, the MJO variance peaks in the northern MC and equatorial MC in ON and AM, respectively (Figs. 2a-c). The MJO precipitation variance averaged in the SMC during DJFM is about 6.34 and 2.30 times higher than that in ON and AM, respectively (Fig. 2d).

While the much weaker MJO variability in the SMC during ON and AM seems to be due to the seasonal shift in the preferred latitude band for MJO propagation, understanding the stark difference in MJO variability in the SMC between DJFM and its two shoulder seasons may provide useful insight into the mechanism that is responsible for the southward MJO detour during DJFM. Note that previous studies of the MJO detour (Kim et al. 2017; Zhou and Murtugudde 2020) also focused on December–February (DJF) rather than a broader boreal winter period (November–April). While the focus of the previous studies is the difference between detour events and nondetour events (e.g., Zhou and Murtugudde 2020) or between the propagating and nonpropagating events during boreal winter (e.g., Feng et al. 2015; DeMott et al.

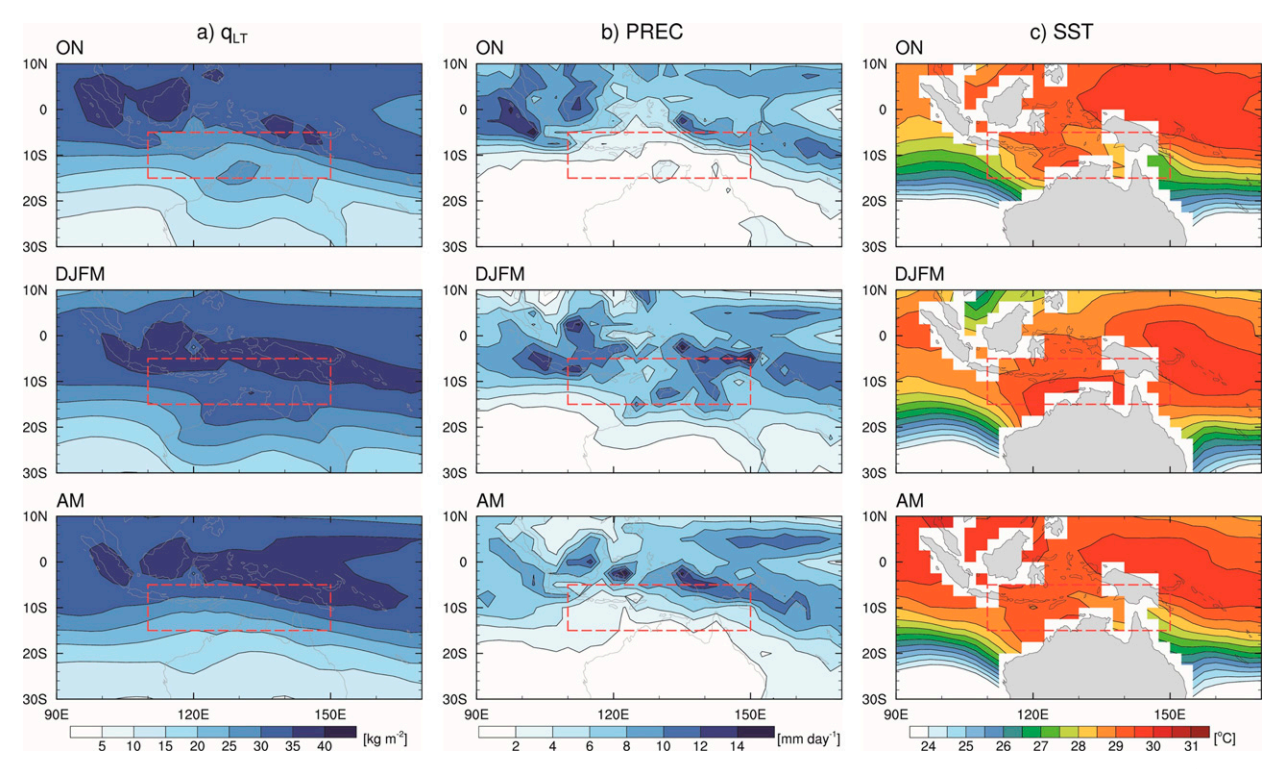


FIG. 3. Climatological mean of (a) low-tropospheric (925–500 hPa) moisture (q_{LT} ; kg m⁻²), (b) precipitation (mm day⁻¹), and (c) SST (°C) for 1998–2018 in each season. The red boxes indicate the SMC region.

2018; Li et al. 2020), we aim to reveal the difference in MJO detour between DJFM and its shoulder seasons by identifying role of the processes that are affected by the mean state.

To explore how the seasonal evolution of the mean state manifests in the SMC region, Fig. 3 compares the geographical distribution of selected mean-state variables among the seasons. Figure 3a shows long-term mean climatology of the lower-free-tropospheric moisture (q_{LT}) , which is specific humidity anomalies integrated from 925 to 500 hPa. We note that moisture variability in these vertical levels have a crucial role on the development of MJO convection (Gonzalez and Jiang 2017). Mean-state q_{LT} in DJFM shows a maximum around 5°S and that higher than 30 kg m⁻² stretches toward northern Australia, indicating a large enough atmospheric moisture contents and an increase in precipitation over the SMC region (Figs. 3a,b). Meanwhile, q_{LT} during ON and AM peaks around the equator with dryer atmosphere and lower precipitation over the SMC than during DJFM. Also shown in Fig. 3 is the mean-state SST. SST in the Timor Sea is relatively warmer in DJFM than that in ON and AM, while SST near the MC islands at the equator is higher in ON and AM (Fig. 3c). The location of the highest SST in each season does not exactly match that of q_{LT} and precipitation, implying that the mean SST itself cannot fully explain the distribution of the mean-state moisture and precipitation.

Inspired by the view that maintenance and propagation of the MJO are explained by moisture anomalies (i.e.,

moisture mode theory; Sobel and Maloney 2012, 2013; Adames and Kim 2016), we test whether the moisture variability alone can explain the seasonality of MJO variability in the SMC. Figure 4 shows the MJO-related variability of $q_{\rm LT}$ anomalies. There is a notable difference in the geographical distribution of MJO precipitation and moisture variability in all seasons. MJO moisture variance tends to maximize at a relatively higher latitude than the MJO precipitation variance. Focusing on the SMC region, unlike the MJO precipitation variance peaking in DJFM (Fig. 2d), the MJO moisture variance is relatively stationary across the seasons (Fig. 4d) and shows no well-defined peak in DJFM. The results shown in Figs. 2 and 4 suggest that the seasonality in MJO precipitation variance in the SMC cannot simply be explained by that in MJO moisture variability. In the following subsections, we investigate the moisture-precipitation coupling and wind-evaporation feedback to understand why a similar moisture variability yields much greater convection variability in DJFM.

b. Role of moisture-precipitation coupling

We first analyze the relationship between $q_{\rm LT}$ and precipitation in the form of a joint histogram between the two variables to see if their relationship varies from one season to another (Figs. 5a-c). Also indicated is the average precipitation as a function of $q_{\rm LT}$ (solid lines in Figs. 5a-c). The overall shape of the joint histogram and the average precipitation value corresponding to a given $q_{\rm LT}$ are almost

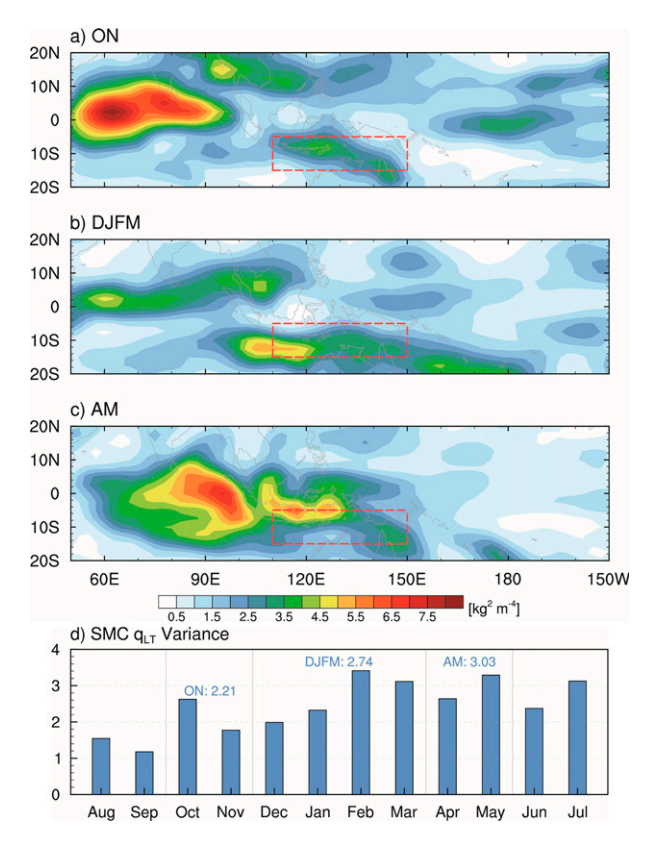


FIG. 4. As in Fig. 2, but for the variance of daily $q_{\rm LT}$ anomalies $({\rm kg^2\,m^{-4}})$.

identical across the seasons in the SMC region. In all seasons, precipitation increases rapidly with $q_{\rm LT}$, especially when $q_{\rm LT}$ is greater than about 35 kg m⁻². This suggests that the underlying moisture–precipitation relationship (e.g., Bretherton et al. 2004; Rushley et al. 2018) does not vary across the seasons. Instead, it is the number of days with $q_{\rm LT}$ higher than 35 kg m⁻² that distinguishes DJFM from ON and AM (Figs. 5a–c). With more frequent moist days, DJFM exhibits a larger mean-state $q_{\rm LT}$ and precipitation (black dots in Figs. 5a–c).

Figures 5d-f show the same joint histograms and average precipitation values as in Figs. 5a-c, except that MJO anomalies are used instead of the raw values. The joint histogram of MJO anomalies in DJFM is clearly different from that in the other seasons; the slope of the average precipitation line is much steeper, indicating that the same amount of MJO moisture anomaly corresponds to a much greater precipitation anomaly in DJFM. Interestingly, the difference between the seasons in the magnitude of the slopes in Figs. 5d-f roughly matches that of the lines that are tangential to the average precipitation curves in Figs. 5a-c at the value of the mean $q_{\rm LT}$. In DJFM, with the high mean $q_{\rm LT}$ (Fig. 3a), perturbations in moisture around the mean value would cause greater changes in precipitation. This suggests that the mean-state moisture difference between the seasons leads to a greater sensitivity of precipitation to moisture in DJFM than in the other seasons.

To quantify the moisture sensitivity of convection and compare it between the seasons, we calculate the "convective relaxation frequency (F_c)" of Adames (2017):

$$F_c = \frac{1}{\overline{\tau}_c}; \quad \overline{\tau}_c = \frac{\langle \overline{q_s} \rangle}{a\overline{P}},$$
 (1)

where $\overline{\tau}_c$ is the convective moisture adjustment time scale, $\langle \overline{q_s} \rangle$ and \overline{P} are the mean-state column-integrated saturation specific humidity and precipitation, respectively. The sensitivity parameter a is obtained by fitting the following equation to daily precipitation and column relative humidity (CRH) data (Bretherton et al. 2004; Rushley et al. 2018):

$$P = P_0 \exp(a \text{CRH}), \tag{2}$$

where $CRH = \langle q \rangle / \langle q_s \rangle$; $\langle q \rangle$ and $\langle q_s \rangle$ are column-integrated specific humidity and saturation specific humidity, respectively; and P_0 is constant. By design, $\overline{\tau_c}$ determines the moisture adjustment time scale of a precipitation response (i.e., $\overline{\tau_c} = \langle q' \rangle / P'$). Then, a higher F_c indicates a faster conversion rate from moisture anomaly to precipitation anomaly (Adames 2017).

Figure 6 shows F_c in the vicinity of the MC calculated in each season. The areas with a higher F_c migrate toward the Southern Hemisphere in DJFM, which resembles the seasonal cycle of the MJO precipitation variance (Fig. 2). F_c averaged in the SMC region during DJFM is 2.46 and 1.57 times higher than that during ON and AM, respectively, which is consistent with the seasonality of the slope between q_{LT} and precipitation anomaly (Figs. 5d-f). The seasonal cycle of F_c suggests that a higher F_c —a more efficient conversion from moisture anomaly to precipitation anomaly—contributes to the stronger MJO precipitation variability in the SMC during DJFM. Figure 6d shows the seasonality of F_c and that of the mean-state variables used for calculating F_c [Eq. (1)]. The seasonal cycle of F_c distribution resembles that of the mean-state precipitation (Fig. 3b), indicating that the seasonal F_c variation in the SMC is a function of mean precipitation, while the mean $\langle q_s \rangle$ remain constant across the seasons (Fig. 6d). This implies the seasonal variation of relative humidity is more likely to be associated with that of column moisture content rather than air temperature. It will be shown later that the seasonal evolution of the mean precipitation in the SMC region is closely associated with the Australian monsoon (Fig. 11).

The results shown in this subsection demonstrate the importance of moisture–precipitation coupling in the seasonal variation of MJO precipitation variance in the SMC. Our findings suggest that the higher mean precipitation in DJFM, which leads to a more efficient conversion from moisture anomaly to precipitation anomaly (i.e., higher F_c), is a critical factor for the exclusively higher MJO precipitation variance in DJFM, despite the relatively stationary MJO moisture variance.

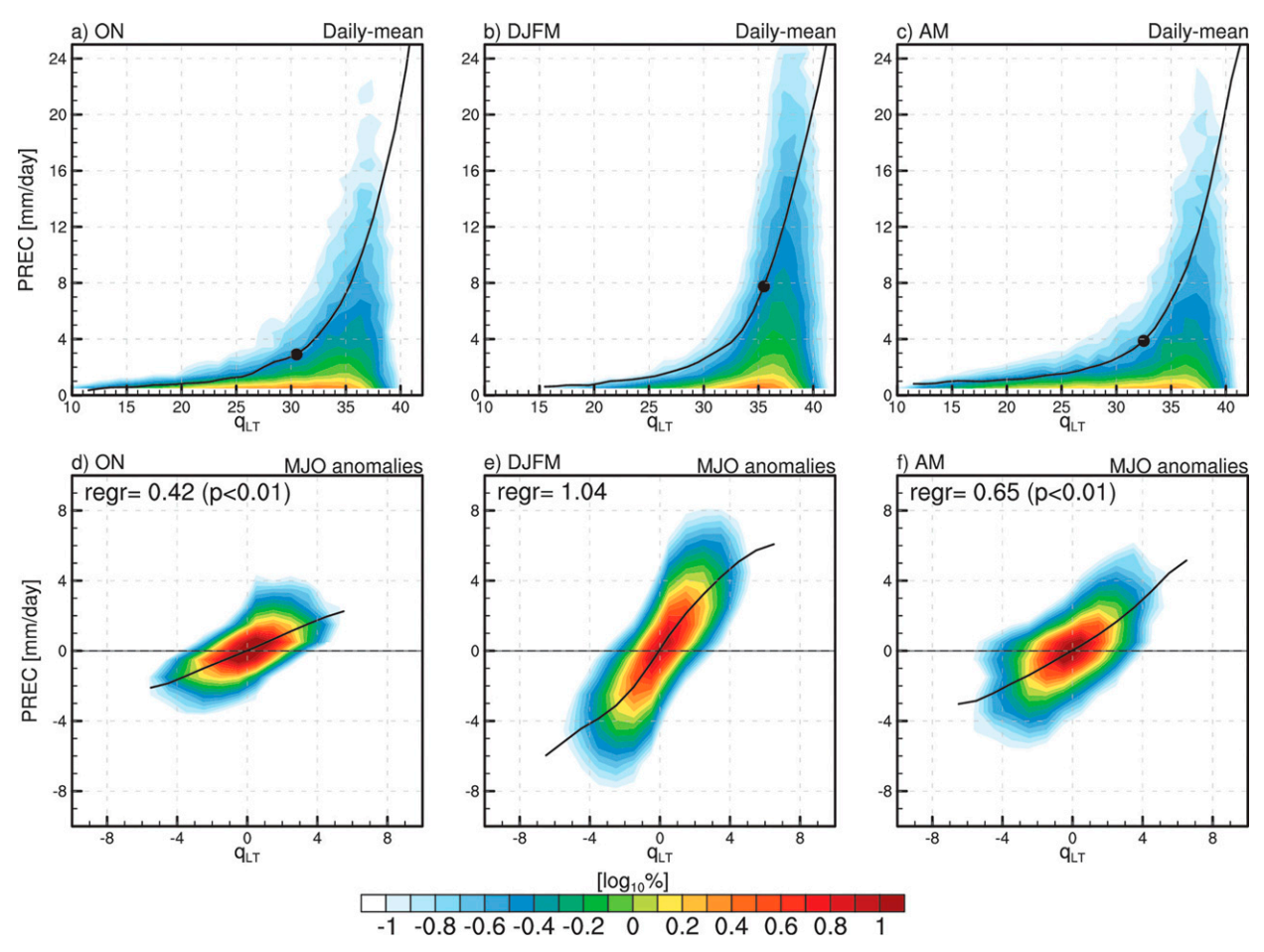


FIG. 5. Joint histogram of daily $q_{\rm LT}$ (kg m⁻²; x axis) and precipitation (mm day⁻¹; y axis) collected over the ocean grid points in the SMC region (15°–5°S, 110°–150°E). (a)–(c) Daily mean and (d)–(f) MJO anomaly. Black solid lines indicate averaged precipitation binned by $q_{\rm LT}$ (results with fewer than 100 samples are omitted). Black dots in (a)–(c) indicate the climatological mean values. In (d)–(f), regression coefficient of average precipitation values onto $q_{\rm LT}$ bins is indicated in the panel, and the p value in the parenthesis indicates significance of the regression coefficient difference from DJFM.

c. Role of wind-evaporation feedback

In this subsection, we examine seasonal variation in the wind-evaporation feedback and the mean-state low-level wind. With the development of organized convection associated with the MJO, upward motion and diabatic heating induce anomalous horizontal circulations approximately in the form of the Matsuno-Gill response (Matsuno 1966; Gill 1980). The circulation anomalies affect surface latent heat flux variability under the organized convection, thereby either positively or negatively feedback on the convection. This wind-evaporation feedback, often referred to as windinduced surface heat exchange (WISHE; Emanuel 1987), has been suggested as a crucial process in the MJO propagation and maintenance (Maloney and Sobel 2004; Lin et al. 2000; Sobel et al. 2010; DeMott et al. 2015; Fuchs and Raymond 2017; Shi et al. 2018; Bui and Maloney 2020). As an example, Maloney and Sobel (2004) showed the magnitude of the wind-evaporation feedback is correlated with

MJO intensity in a series of GCM simulations in which the mixed-layer depth is varied. Sobel et al. (2010) showed that the intraseasonal variability of precipitation and surface latent heat flux locally coexist, which are evident in both observations and a global model simulation. Fuchs and Raymond (2017) presented a simple model for the MJO in which WISHE plays an essential role in the MJO-like variability. Although many of the studies suggested a crucial role for wind–evaporation feedbacks in simulated MJOs, the details of the wind–evaporation feedback varied from model to model, and their relevance to observations remains a key issue. In the following, we investigate whether and how wind–evaporation feedbacks promote the MJO's southward detour during boreal winter.

Figure 7 compares the joint histogram of daily near-surface zonal wind and surface latent heat flux over the SMC region between the seasons. As expected, latent heat flux is larger when the magnitude of zonal wind (i.e., wind speed) is stronger (Figs. 7a-c). Note that the wind variation in the zonal

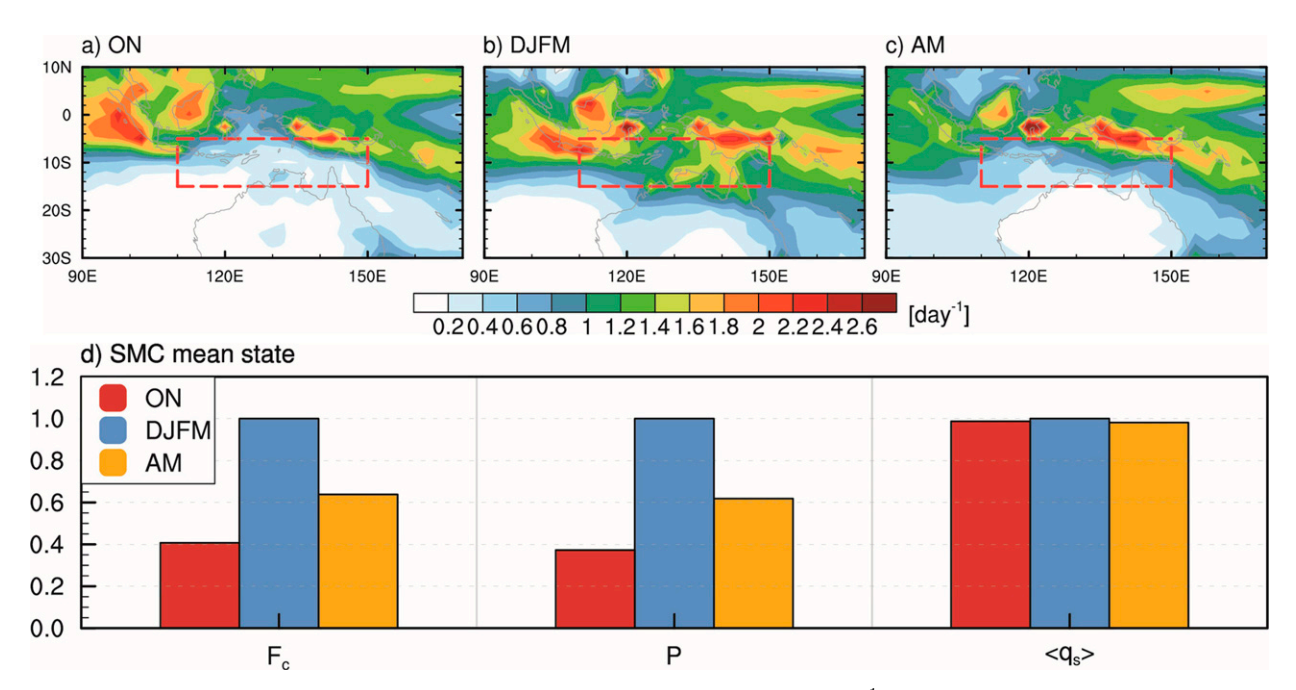


FIG. 6. (a)–(c) Climatological mean of the convective relaxation frequency (F_c ; day⁻¹) for 1998–2018 in each season. The red boxes indicate the SMC region. (d) Area-average of climatological F_c , precipitation, and column-integrated saturation specific humidity in the SMC region. To see relative changes of the variables between seasons, each variable in (d) is normalized by the value in DJFM.

direction dominates the total wind speed in this region (not shown). While the majority of near-surface zonal wind in DJFM are westerly, easterlies are more frequently observed in ON and AM. Indeed, the mean-state zonal wind in DJFM is westerly, and that in ON and AM is easterly (black dots in Figs. 7a–c).

Figure 8 shows the geographical distribution of the background near-surface zonal wind in each season. In DJFM, the background westerlies are dominant to the south of the equator in the eastern Indian Ocean and the MC (Fig. 8b). On the contrary, the direction of the background zonal wind in the SMC region is mostly weak easterly during ON, and these background easterlies are even more dominant during AM (Figs. 8a,c). For the MJO anomalies of the joint histogram, it seems the direction of the background zonal wind determines the relationship between zonal wind and latent heat flux (Figs. 7d-f). In DJFM, with the background westerlies, the MJO latent heat flux anomalies tend to increase with the positive MJO zonal wind (i.e., westerly) anomalies. On the contrary, latent heat flux anomalies tend to decrease with the positive zonal wind anomalies in AM and to a lesser degree in ON.

Figure 9 shows the MJO anomalies of near-surface zonal wind and latent heat flux as a function of MJO precipitation anomalies. The active convective regions associated with the MJO tend to exhibit westerly wind anomalies regardless of the seasons (Figs. 9a–c). In DJFM, the westerly MJO anomalies are superimposed on background westerlies, leading to a positive correlation between precipitation and latent heat flux anomalies (r = 0.55; Fig. 9e) that is statistically significant at

the 99% confidence level. The positive correlation between precipitation and latent heat flux anomalies indicates that wind-evaporation feedback works toward enhancing MJO precipitation variability under the moisture mode paradigm (e.g., Adames and Kim 2016). However, in ON and AM, with the background easterlies, MJO precipitation anomalies exhibit little correlation (ON) or are negatively (AM) correlated with MJO latent heat flux anomalies, indicating a weak (ON) or negative wind-evaporation feedback (Figs. 9d,f).

To further examine the wind-evaporation feedback during the MJO's life cycle, MJO phase composites of zonal wind, vertical velocity, precipitation, and surface latent heat flux anomalies are compared (Fig. 10). The MJO precipitation anomalies over the SMC peak around phase 5 with westerly (easterly) anomalies in the lower (upper) troposphere, regardless of the seasons. The peak of anomalous upward motion (phase 5), which corresponds to anomalous precipitation, lags by one phase that of the low-level zonal wind convergence (phase 4). This lag reveals that the low-level convergence is located at the east of the MJO convection center during its eastward propagation, indicating the anomalous westerlies present at the peak of anomalous precipitation (phase 5).

In contrast to the consistent structures of precipitation and atmospheric circulation in their phase composites, latent heat flux anomalies exhibit different behaviors among the seasons. With the weak MJO variability and background zonal wind during ON, only subtle wind–evaporation feedbacks are present over the SMC region (Fig. 10a). On the

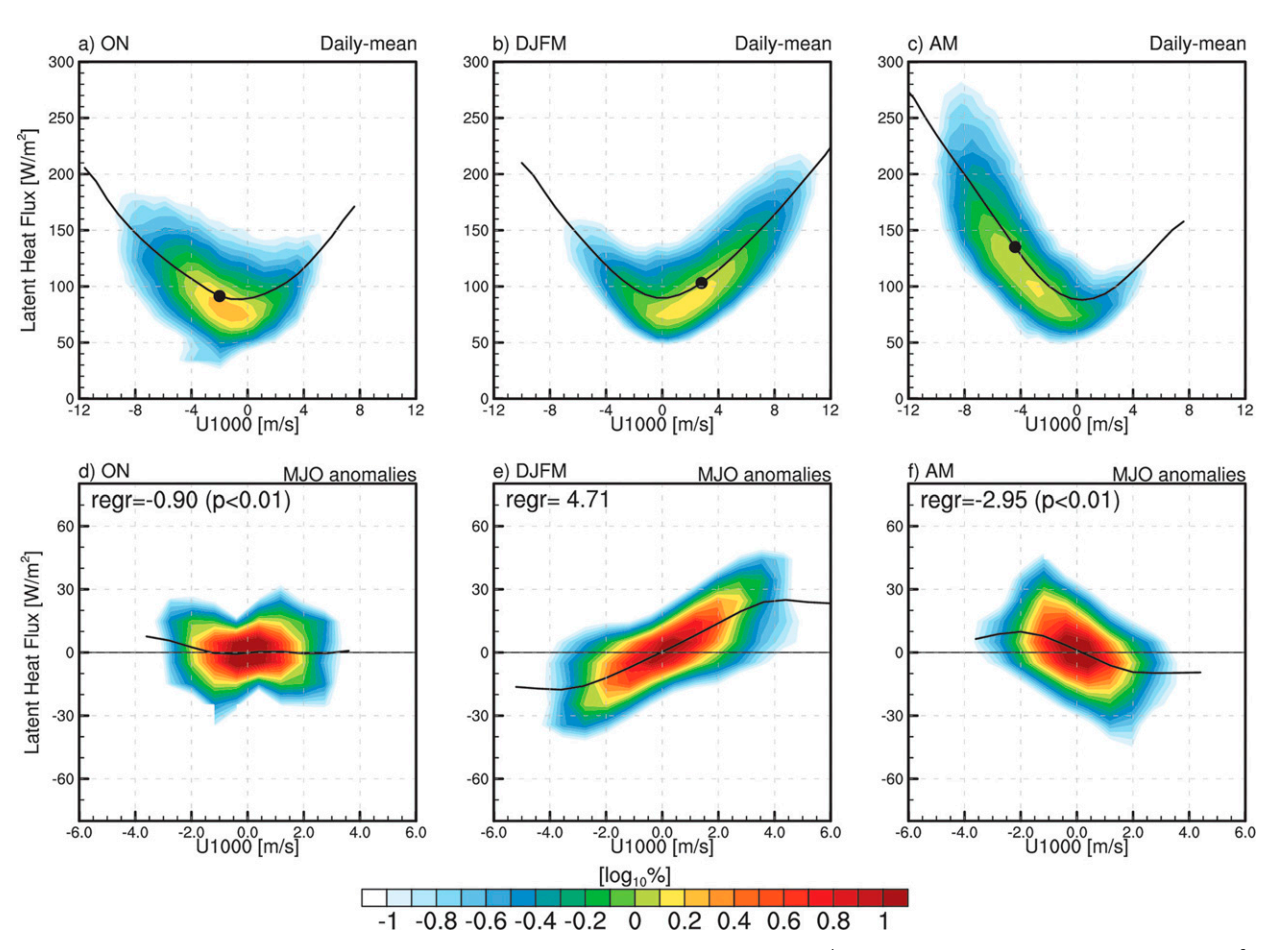


FIG. 7. As in Fig. 5, but for the joint histogram of daily zonal wind at 1000 hPa (m s⁻¹; x axis) and surface latent heat flux (W m⁻²; y axis). In (d)–(f), regression coefficient of average latent heat flux values onto the zonal wind bins is indicated in the panel, and the p value in the parenthesis indicates significance of the regression coefficient difference from DJFM.

other hand, wind-evaporation feedbacks are prominent during DJFM and AM with the strong background westerlies and easterlies, respectively (Figs. 10b,c). The westerly wind anomalies during the active convection (phases 5 and 6) are superimposed on the background westerly (easterly) in DJFM (AM), increasing (decreasing) total wind speed and

latent heat flux (Figs. 10b,c). The role of positive wind-evaporation feedback described in this study is consistent with the mechanism proposed by Zhou and Murtugudde (2020), who emphasized that the detour events are accompanied by the prominent westerly wind anomalies over the SMC. Our results indicate that the wind-evaporation

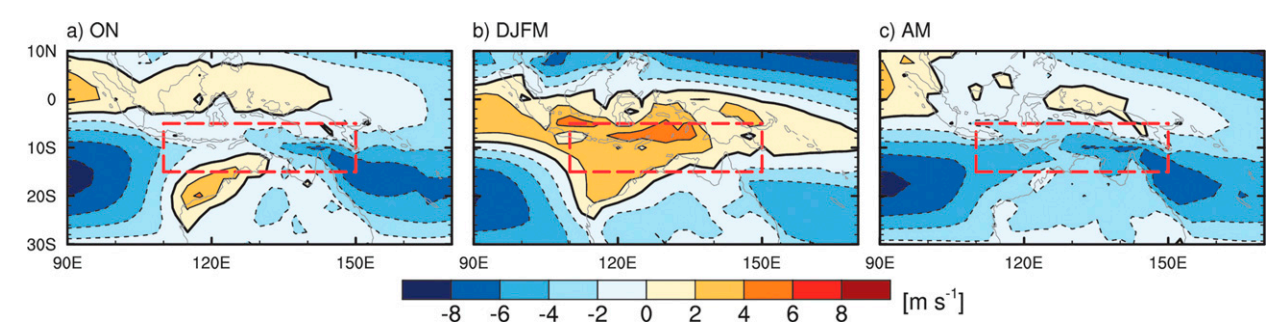


FIG. 8. Climatological mean of zonal wind at 1000 hPa (m s⁻¹) in (a) ON, (b) DJFM, and (c) AM. The red boxes indicate the SMC region. Thin solid and dashed contours indicate positive and negative anomalies, respectively, and the zero line is indicated with the thick solid line.

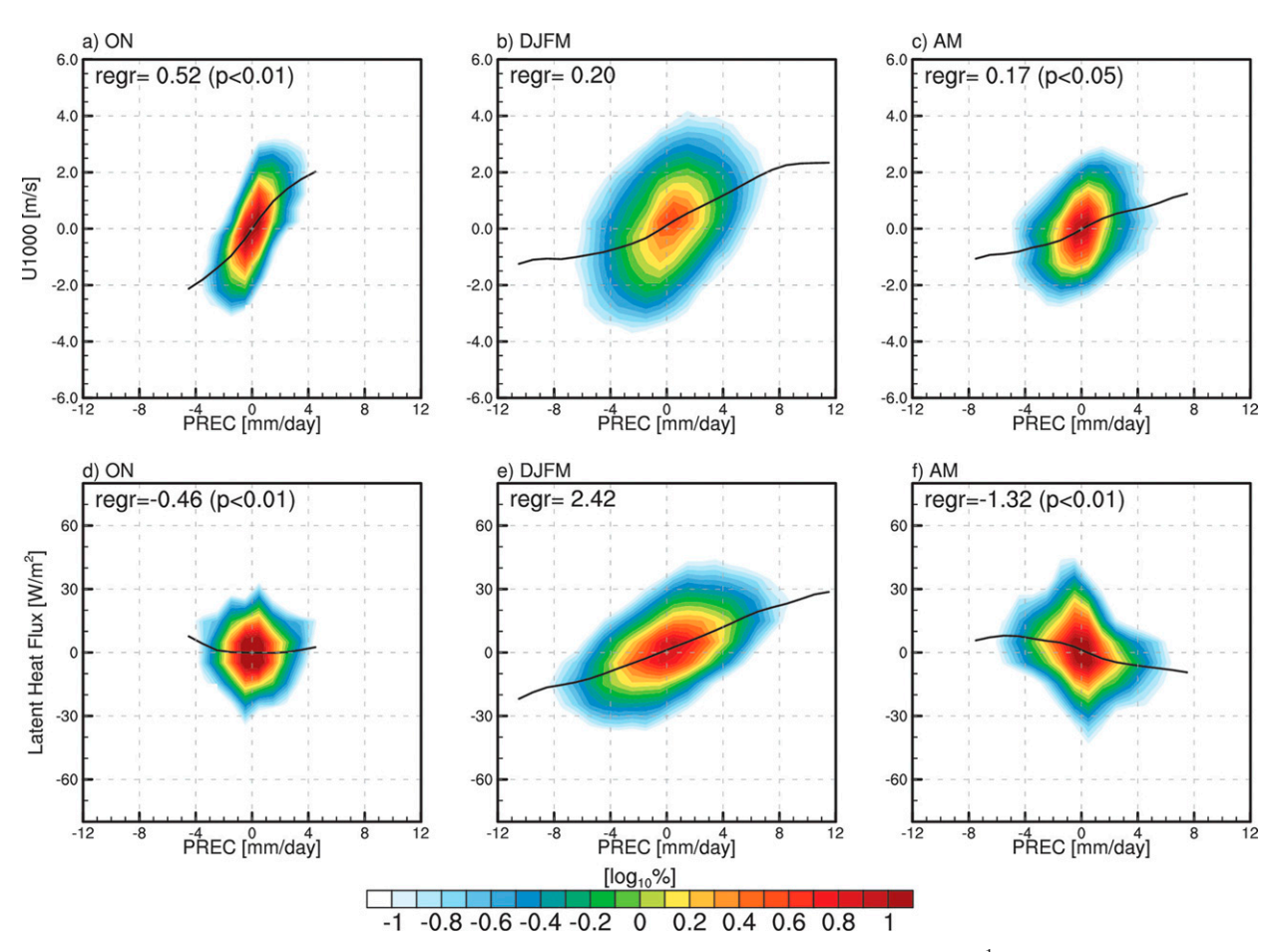


FIG. 9. (a)–(c) As in Figs. 5d–f, but for the joint histogram of daily MJO precipitation anomaly (mm day⁻¹; x axis) and MJO zonal wind anomaly at 1000 hPa (m s⁻¹; y axis). (d)–(f) As in (a)–(c), but for the joint histogram of daily MJO precipitation anomaly (mm day⁻¹; x axis) and the MJO surface latent heat flux anomaly (W m⁻²; y axis). Regression coefficient of average zonal wind and latent heat flux values onto precipitation bins is indicated in the panel, and the p value in the parenthesis indicates significance of the regression coefficient difference from DJFM.

feedback plays a critical role exclusively in DJFM, which is facilitated by the mean-state westerlies that are absent in other seasons.

The results shown in this subsection highlight a possible role for wind-evaporation feedback on supporting the seasonal variation of MJO moisture variance, which then could affect MJO precipitation variance via moisture-precipitation coupling in the SMC. In DJFM, the higher variances of moisture and precipitation coexist over the ocean in the SMC (Figs. 2b and 4b), which indicates the supportive role of wind-evaporation feedback in addition to the moisture-precipitation coupling. In particular, our results suggest that the background westerlies are a mean-state parameter that favors MJO development over the SMC exclusively during DJFM by modulating the magnitude and sign of the wind-evaporation feedback.

d. Role of the Australian monsoon

In this section, motivated by the important role of the mean-state variables underscored in sections 3b and 3c, we

focus on how the background state fosters the MJO's southward detour in DJFM. To illustrate the association of the mean-state variables highlighted above with MJO variability during the climatological seasonal cycle, Fig. 11 shows the seasonal evolution of four mean-state variables together with that of MJO precipitation variance in the SMC region. The convective relaxation frequency (F_c) and MJO precipitation variance show a robust linear relationship (r = 0.95; Fig. 11a). One interesting feature in Fig. 11a is the sharp increase from November to December in both variables, which is associated with the onset of the Australian monsoon. At the beginning of the austral summer, differential heating between land and ocean leads to a rapid development of precipitation over the northern Australia land area from November to December (Fig. 11b). With the monsoon precipitation developed in northern Australia, low-level northwesterlies near and to the north of Australia associated with a southward shift of the local Hadley circulation transport warm and moist air from the Indian Ocean (Fig. 12; e.g., Kim et al. 2006), increasing moisture and

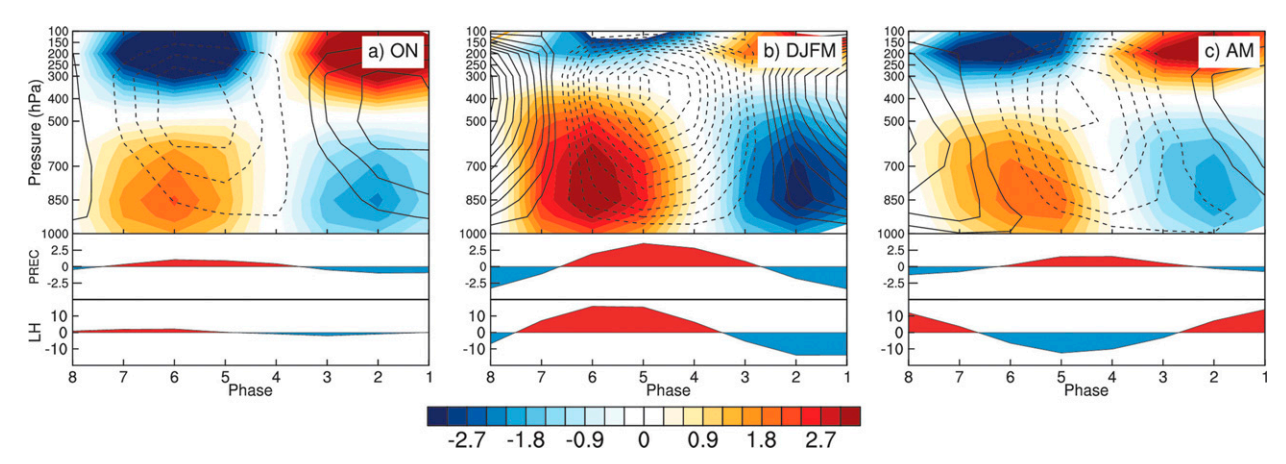


FIG. 10. (top) MJO life cycle composite of MJO zonal wind (shaded; m s⁻¹) and vertical velocity (contours; Pa s⁻¹) anomalies averaged in the SMC region (ocean only; 15° – 5° S, 110° – 150° E) obtained from each MJO phase (RMM amplitude > 1). Contour interval is 0.003 Pa s⁻¹, and solid and dashed contours correspond to positive and negative anomalies, respectively. Zero line is omitted. (middle),(bottom) The graphs below show the composite of MJO precipitation (mm day⁻¹) and surface latent heat flux anomalies (W m⁻²), respectively. Note that the *x* axis (MJO phase) is reversed.

precipitation over the SMC during the Australian monsoon period (Figs. 3a,b, 11a). The seasonal locking of the Australian monsoon is associated with the meridional migration of the Hadley circulation, which is ultimately tied to the climatological seasonal cycle of insolation. Our study focused on the features of the Australian monsoon system that are part of the climatological seasonal cycle and our results suggest that the rapid seasonal transition of the MJO behavior during austral summer also follows the onset and decay of the Australian monsoon in the climatological seasonal cycle. It should be noted that, although the Australian monsoon is a seasonally locked phenomenon, the exact timing of its onset and demise varies from one year to another due to internal variability; it has been shown that the timing of the Australian monsoon onset each year is affected by the intraseasonal variability, and the onset occurs mostly in the active phase of the MJO (Wheeler and Hendon 2004; Duan et al. 2019).

The onset of the Australian monsoon is also manifest in a reversal of low-level wind direction (Hung and Yanai 2004). The Australian monsoon index, defined by the lowlevel zonal wind in the north of Australia (Kajikawa et al. 2010), and the near-surface zonal wind over the SMC both exhibit a rapid transition from easterlies to westerlies during the onset from November to December, and vice versa during the withdrawal from March to April (Figs. 11c,d, 12). This zonal wind variability also exhibits a robust linear relationship with the MJO precipitation variance, revealing that the Australian monsoon provides a mean state favorable for MJO development. We argue that the Australian monsoon affects MJO precipitation variance in the SMC by modulating the mean precipitation and lowlevel zonal wind, which affect moisture-precipitation coupling and wind-evaporation feedback, respectively. In general, the Australian monsoon is known to be predominant during DJFM (Kajikawa et al. 2010; Drosdowsky 1996),

which is consistent with the argument proposed in this study.

Figure 13 summarizes the mean-state changes accompanied by the Australian monsoon and how they affect MJO development in the SMC region. In DJFM, low-level northwesterly winds transport moisture into the SMC and northern Australia from the equator (Fig. 13a). The larger mean precipitation and westerly wind within the active Australian monsoon provide a favorable state for the MJO to detour into the SMC. On the other hand, in ON and AM, southeasterly mean winds allow the SMC to dry, inhibiting the development of MJO convection in this region (Fig. 13b).

4. Summary and conclusions

Motivated by the limited understanding of why the major convective envelope of the MJO detours to the south of the MC only during boreal winter (DJFM), this study examined the processes that explain the seasonal locking of the MJO's southward detour. Precipitation and moisture variability associated with the MJO, the moisture-precipitation relationship, and wind-evaporation feedbacks were compared between DJFM and its shoulder seasons (ON and AM) in the SMC region, with a special emphasis on the role of the mean state. Note that we also examined longwave cloud-radiation feedback (Lin and Mapes 2004; Andersen and Kuang 2012; Kim et al. 2015) and other mean-state variables such as the "alpha" parameter defined by Chikira (2014) and found that they did not show notable difference among the seasons (not shown).

We first tested whether the moisture variability alone can explain the seasonality of MJO variability in the SMC. MJO-related variance of precipitation and low to midtropospheric moisture anomalies in DJFM were compared

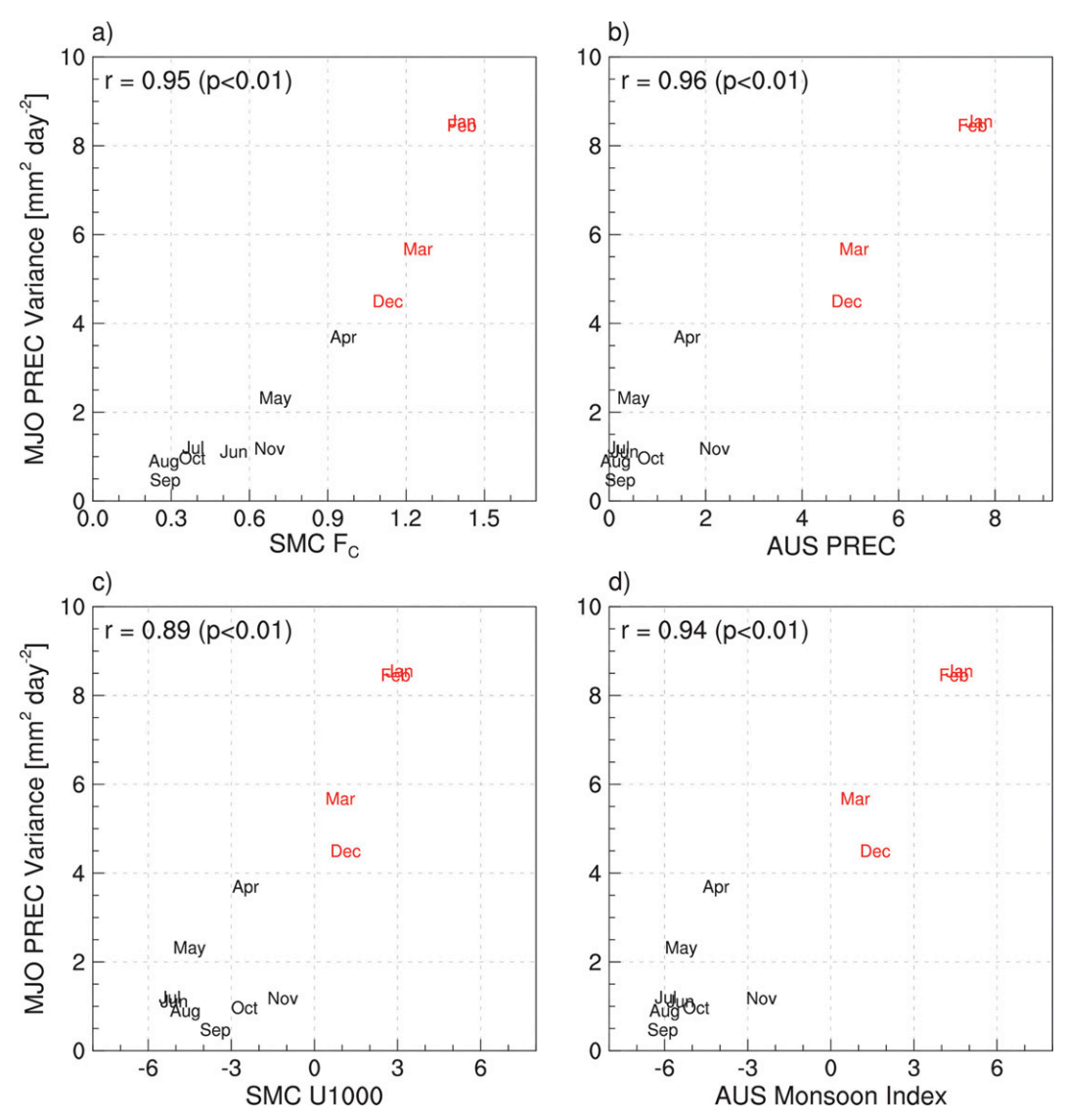


FIG. 11. Scatterplot of (a) F_c (day⁻¹), (b) area-averaged precipitation (mm day⁻¹) in the northern Australia land area (20°-10°S, 110°-150°E), (c) zonal wind at 1000 hPa (m s⁻¹) in the SMC, and (d) the Australian monsoon index (m s⁻¹, Kajikawa et al. 2010) (x axis) with MJO precipitation variance (y axis) averaged in the SMC region within the climatological seasonal cycle. DJFM and the other months are marked with red and black, respectively.

with those in the seasons before (ON) and after (AM). While MJO precipitation variance over the SMC was found to be much larger during DJFM than the other seasons, MJO moisture variance was comparable among the seasons, revealing an existence of processes enhancing precipitation variability within the nearly constant moisture variability.

The relationship between free-tropospheric moisture and precipitation in the SMC region was then examined and compared among the seasons in the form of the joint histogram. In the total field, there was no discernable difference between the seasons; similar moisture values corresponded to similar precipitation values with the well-known exponential-like

relationship between the two (Bretherton et al. 2004; Rushley et al. 2018). In MJO anomalies, however, the same moisture anomaly in DJFM was found to be associated with a larger precipitation anomaly than in the other seasons, suggesting a greater moisture sensitivity of precipitation in DJFM. This seems at least partly responsible for the seasonal cycle of MJO precipitation variance peaking in DJFM despite of the relatively small seasonality of the moisture variance. Given the exponential-like relationship between moisture and precipitation in the total field, the larger mean-state precipitation and moisture in DJFM causes the moisture sensitivity of precipitation (F_c) higher during that season. It was also shown that F_c and MJO precipitation variance

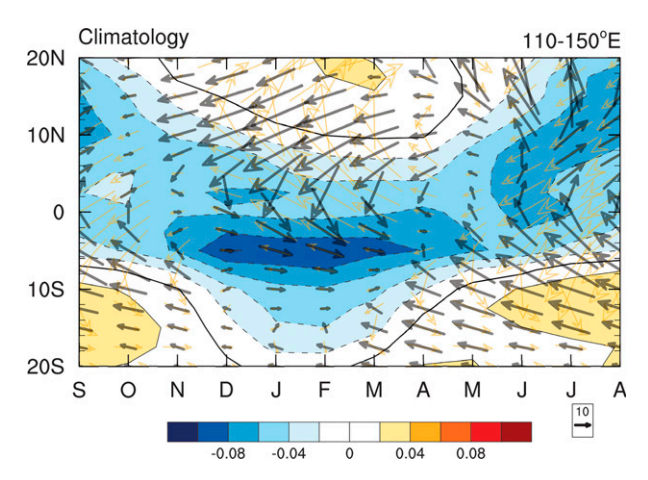


FIG. 12. Climatological seasonal cycle for 1998–2018 at each month (x axis) of circulation variables zonally averaged between 110° and 150°E. Shading shows omega (Pa s⁻¹) at 500 hPa. Black and yellow arrows indicate wind vectors (m s⁻¹) at 850 and 200 hPa, respectively. For enhanced readability, the wind magnitude at 850 hPa is multiplied by 2. Additionally, meridional wind in all levels is multiplied by 5.

covary within the climatological seasonal cycle, suggesting that the increase in the mean-state precipitation and moisture is a key factor for the southward detour of MJO convection in DJFM.

The role of wind-evaporation feedback to the development of MJO convection in the SMC region was also examined. The total field surface latent heat flux is proportional to the speed of the near-surface zonal wind, a relationship consistent among the seasons. Because the total wind speed is largely determined by the sum of the background zonal wind and its anomaly, the mean-state zonal wind determines the relationship between the zonal wind anomaly and latent heat flux anomaly. Regardless of the seasons, westerly anomalies are present in the lower troposphere near the center of MJO convection. The westerly anomalies are superimposed on the background westerlies in DJFM, yielding an increase in latent heat flux. The enhanced latent heat flux supplies additional water vapor to MJO convection, contributing to the maintenance of the convection (i.e., positive wind-evaporation feedback). However, westerly anomalies in background easterlies in the other seasons leads to a negative wind-evaporation feedback. The contrast in the sign of the wind-evaporation feedback on MJO maintenance among the seasons suggests that the mean-state westerlies in DJFM are a crucial factor for the MJO's southward detour during that season.

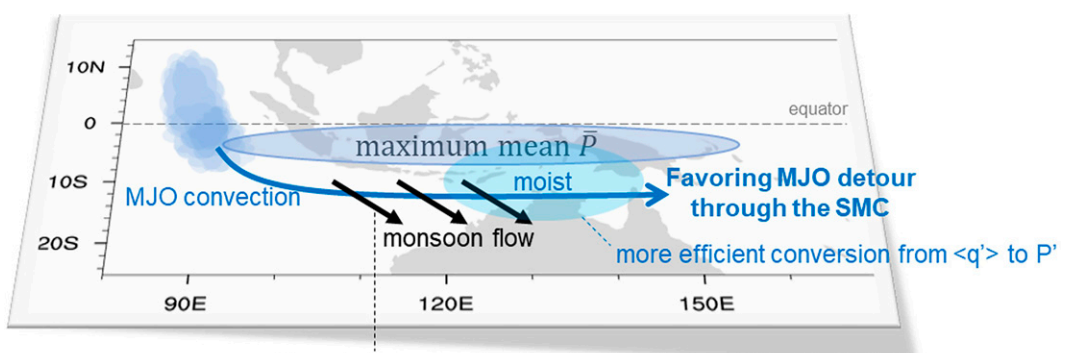
The mean-state conditions that critically affect the development of MJO convection in the SMC through moisture–precipitation coupling and wind–evaporation feedbacks were found to be closely linked to the Australian monsoon. During the Australian monsoon season, low-level northwesterly winds transport moist air masses to the SMC and northern Australia from the equator, which increases the mean precipitation and moisture, enhancing moisture–precipitation

coupling. The westerly component of the mean wind that arises during monsoon onset changes the sign of the windevaporation feedback from negative to positive. The monthly seasonal cycle of MJO precipitation variance in the SMC region and the important mean-state factors regulating such variance closely follow that of the Australian monsoon, which is active exclusively in DJFM. The robust correlation of MJO activity and mean-state evolution strongly suggests that the MJO's southward detour occurs preferentially when the Australian monsoon system fosters the mean state favorable for MJO maintenance. In a companion study (Rushley et al. 2022, manuscript submitted to J. Climate), we examine the seasonal cycle of MJO activity in GCM simulations in which the orbital parameters are altered and find that the moisture-convection coupling and windevaporation feedback play a critical role in the simulation of the MJO's seasonality.

Also, the onset and intensity of the Australian monsoon vary with low-frequency variability such as El Niño-Southern Oscillation (Kajikawa et al. 2010; Lisonbee and Ribbe 2021), implying that interannual and interdecadal variations of intensity and timing of the Australian monsoon could affect the MJO detour. The distribution of the mean-state moisture gradient, which has been suggested as a crucial factor for variability in MJO propagation across the MC at interannual (Kang et al. 2021) and interdecadal time scales (Kang et al. 2020), is likely associated with the Australian monsoon. MJO diversity (Wang et al. 2019) and the phase speed of MJO propagation (e.g., Chen and Wang 2020) may also be affected by whether an MJO event occurs in the season with or without the active Australian monsoon. These aspects warrant further investigations of the relationship between the Australian monsoon and the MJO.

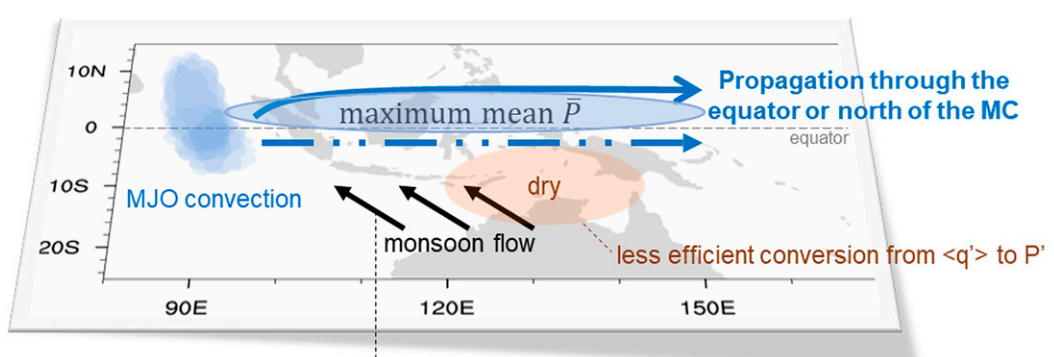
Because many contemporary climate models fail to simulate realistic MJO propagation (Jiang et al. 2015; Ahn et al. 2020b), it is uncertain whether these models are able to simulate the seasonal cycle of the southward detour realistically. Future investigations of how mean-state bias associated with the Australian monsoon affect models' ability to simulate the southward detour are warranted. Also, the direction of projected change in the Australian monsoon precipitation with warming remains uncertain, with a nearly equal number of climate models projecting increases and decreases in land precipitation over the northern Australia, despite the reduced model spread in phase 6 of the Coupled Model Intercomparison Project (CMIP6) compared to that in CMIP5 (Dey et al. 2019; Jin et al. 2020; Narsey et al. 2020). Projected model changes to the MJO under the warming also show considerable intermodel spread (Maloney et al. 2019; Rushley et al. 2019), some of which may be related to the uncertainties in the Australian monsoon change. Improved process understanding of the relationship between the Australian monsoon and MJO may help engender improvements in global climate models (GCMs) to produce more accurate simulations of MJO propagation and teleconnections.

a) DJFM



positive wind-evaporation feedbacks with background westerlies

b) ON & AM



negative wind-evaporation feedbacks with background easterlies

FIG. 13. A schematic diagram summarizing the role of the Australian monsoon in the MJO's southward detour across the MC. (a) In the active Australian monsoon period (DJFM), the northwesterly monsoon flow in the lower troposphere transports moisture from the equator to SMC, supporting larger mean precipitation that leads to more efficient conversion from anomalous moisture to anomalous precipitation. Additionally, the background westerlies promote MJO maintenance via positive wind–evaporation feedback. (b) During the two shoulder seasons (ON and AM), the dryer condition and the background easterlies provide an unfavorable condition for MJO development in the SMC region.

Acknowledgments. This work was funded by the NOAA CVP program (NA18OAR4310300; NA18OAR4310299), the DOE RGMA program (DE-SC0016223), the NASA MAP (80NSSC17K0227) and CYGNSS (80NSSC21K1004) programs, and KMA R&D program (KMI2021-01210). This work was also supported by the Sejong Science Fellowship (NRF-2021R1C1C2004621) and the Brain Pool program funded by the Ministry of Science and ICT through the National Research Foundation of Korea (NRF-2021H1D3A2A01039352).

Data availability statement. The sources for data used in this study are as follows: TRMM (https://gpm.nasa.gov/data/directory), ERA5 (https://www.ecmwf.int/en/forecasts/datasets/reanalysis-datasets/era5), HadISST (https://www.metoffice.gov.uk/hadobs/hadisst/), and RMM index (http://www.bom.gov.au/climate/mjo/graphics/rmm.74toRealtime.txt).

REFERENCES

- Adames, Á. F., 2017: Precipitation budget of the Madden–Julian oscillation. J. Atmos. Sci., 74, 1799–1817, https://doi.org/10.1175/JAS-D-16-0242.1.
- —, and J. M. Wallace, 2014: Three-dimensional structure and evolution of the vertical velocity and divergence fields in the MJO. J. Atmos. Sci., 71, 4661–4681, https://doi.org/10.1175/ JAS-D-14-0091.1.
- —, and D. Kim, 2016: The MJO as a dispersive, convectively coupled moisture wave: Theory and observations. *J. Atmos. Sci.*, 73, 913–941, https://doi.org/10.1175/JAS-D-15-0170.1.
- Ahn, M.-S., D. Kim, Y.-G. Ham, and S. Park, 2020a: Role of Maritime Continent land convection on the mean state and MJO propagation. *J. Climate*, 33, 1659–1675, https://doi.org/ 10.1175/JCLI-D-19-0342.1.
- —, and Coauthors, 2020b: MJO propagation across the Maritime Continent: Are CMIP6 models better than CMIP5 models?

- Geophys. Res. Lett., 47, e2020GL087250, https://doi.org/10.1029/2020GL087250.
- Andersen, J. A., and Z. Kuang, 2012: Moist static energy budget of MJO-like disturbances in the atmosphere of a zonally symmetric aquaplanet. *J. Climate*, 25, 2782–2804, https:// doi.org/10.1175/JCLI-D-11-00168.1.
- Bretherton, C. S., M. E. Peters, and L. E. Back, 2004: Relationships between water vapor path and precipitation over the tropical oceans. *J. Climate*, 17, 1517–1528, https://doi.org/10.1175/1520-0442(2004)017<1517:RBWVPA>2.0.CO;2.
- Bui, H. X., and E. D. Maloney, 2020: Changes to the Madden–Julian oscillation in coupled and uncoupled aquaplanet simulations with 4xCO₂. *J. Adv. Model. Earth Syst.*, **12**, e2020MS00217, https://doi.org/10.1029/2020MS002179.
- Chen, G., and B. Wang, 2020: Circulation factors determining the propagation speed of the Madden–Julian oscillation. J. Climate, 33, 3367–3380, https://doi.org/10.1175/JCLI-D-19-0661.1.
- Chikira, M., 2014: Eastward-propagating intraseasonal oscillation represented by Chikira–Sugiyama cumulus parameterization. Part II: Understanding moisture variation under weak temperature gradient balance. J. Atmos. Sci., 71, 615–639, https:// doi.org/10.1175/JAS-D-13-038.1.
- DeMott, C. A., N. P. Klingaman, and S. J. Woolnough, 2015: Atmosphere-ocean coupled processes in the Madden-Julian oscillation. *Rev. Geophys.*, 53, 1099–1154, https://doi.org/10. 1002/2014RG000478.
- —, B. O. Wolding, E. D. Maloney, and D. A. Randall, 2018: Atmospheric mechanisms for MJO decay over the Maritime Continent. J. Geophys. Res. Atmos., 123, 5188–5204, https://doi.org/10.1029/2017JD026979.
- Dey, R., S. C. Lewis, J. M. Arblaster, and N. J. Abram, 2019: A review of past and projected changes in Australia's rainfall. Wiley Interdiscip. Rev.: Climate Change, 10, e577, https://doi. org/10.1002/wcc.577.
- Dole, R., and Coauthors, 2014: The making of an extreme event: Putting the pieces together. *Bull. Amer. Meteor. Soc.*, **95**, 427–440, https://doi.org/10.1175/BAMS-D-12-00069.1.
- Drosdowsky, W., 1996: Variability of the Australian summer monsoon at Darwin: 1957–1992. *J. Climate*, **9**, 85–96, https://doi.org/10.1175/1520-0442(1996)009<0085:VOTASM>2.0.CO;2.
- Duan, Y., H. Liu, W. Yu, L. Liu, G. Yang, and B. Liu, 2019: The onset of the Indonesian–Australian summer monsoon triggered by the first-branch eastward-propagating Madden–Julian oscillation. *J. Climate*, 32, 5453–5470, https://doi.org/10.1175/JCLI-D-18-0513.1.
- Emanuel, K. A., 1987: An air–sea interaction model of intraseasonal oscillations in the tropics. *J. Atmos. Sci.*, **44**, 2324–2340, https://doi.org/10.1175/1520-0469(1987)044<2324: AASIMO>2.0.CO;2.
- Feng, J., T. Li, and W. Zhu, 2015: Propagating and nonpropagating MJO events over Maritime Continent. *J. Climate*, **28**, 8430–8449, https://doi.org/10.1175/JCLI-D-15-0085.1.
- Fuchs, Ž., and D. J. Raymond, 2017: A simple model of intraseasonal oscillations. J. Adv. Model. Earth Syst., 9, 1195–1211, https://doi.org/10.1002/2017MS000963.
- Gill, A. E., 1980: Some simple solutions for heat-induced tropical circulation. *Quart. J. Roy. Meteor. Soc.*, **106**, 447–462, https:// doi.org/10.1002/qj.49710644905.
- Gonzalez, A. O., and X. Jiang, 2017: Winter mean lower tropospheric moisture over the Maritime Continent as a climate model diagnostic metric for the propagation of the Madden-Julian oscillation. *Geophys. Res. Lett.*, 44, 2588–2596, https://doi.org/10.1002/2016GL072430.

- Hersbach, H., and Coauthors, 2019: Global reanalysis: Goodbye ERA-Interim, hello ERA5. ECMWF Newsletter, No. 159, ECMWF, Reading, United Kingdom, 2–10, https://www.ecmwf. int/sites/default/files/elibrary/2019/19027-global-reanalysis-goodbye-era-interim-hello-era5.pdf.
- Huffman, G. J., and Coauthors, 2007: The TRMM Multisatellite Precipitation Analysis (TMPA): Quasi-global, multiyear, combined-sensor precipitation estimates at fine scales. J. Hydrometeor., 8, 38–55, https://doi.org/10.1175/JHM560.1.
- Hung, C.-W., and M. Yanai, 2004: Factors contributing to the onset of the Australian summer monsoon. *Quart. J. Roy. Meteor. Soc.*, 130, 739–758, https://doi.org/10.1256/qj.02.191.
- Jiang, X., and Coauthors, 2015: Vertical structure and physical processes of the Madden-Julian oscillation: Exploring key model physics in climate simulations. *J. Geophys. Res. Atmos.*, 120, 4718–4748, https://doi.org/10.1002/2014JD022375.
- —, and Coauthors, 2020: Fifty years of research on the Madden-Julian oscillation: Recent progress, challenges, and perspectives. J. Geophys. Res. Atmos., 125, e2019JD030911, https://doi.org/10.1029/2019JD030911.
- Jin, C., B. Wang, and J. Liu, 2020: Future changes and controlling factors of the eight regional monsoons projected by CMIP6 models. J. Climate, 33, 9307–9326, https://doi.org/10.1175/ JCLI-D-20-0236.1.
- Kajikawa, Y., B. Wang, and J. Yang, 2010: A multi-time scale Australian monsoon index. *Int. J. Climatol.*, 30, 1114–1120, https://doi.org/10.1002/joc.1955.
- Kang, D., D. Kim, M. Ahn, R. Neale, J. Lee, and J. Peter, 2020: The role of the mean state on MJO simulation in CESM2 ensemble simulation. *Geophys. Res. Lett.*, 47, e2020GL089824, https://doi.org/10.1029/2020GL089824.
- —, —, M.-S. Ahn, and S.-I. An, 2021: The role of background meridional moisture gradient on the propagation of the MJO over the Maritime Continent. *J. Climate*, **34**, 6565–6581, https://doi.org/10.1175/JCLI-D-20-0085.1.
- Kerns, B. W., and S. S. Chen, 2016: Large-scale precipitation tracking and the MJO over the Maritime Continent and Indo-Pacific warm pool. *J. Geophys. Res. Atmos.*, 121, 8755– 8776, https://doi.org/10.1002/2015JD024661.
- Kessler, W. S., 2001: EOF representations of the Madden–Julian oscillation and its connection with ENSO. *J. Climate*, **14**, 3055–3061, https://doi.org/10.1175/1520-0442(2001)014<3055: EROTMJ>2.0.CO;2.
- Kim, D., J. S. Kug, and A. H. Sobel, 2014: Propagating versus nonpropagating Madden–Julian oscillation events. *J. Climate*, 27, 111–125, https://doi.org/10.1175/JCLI-D-13-00084.1.
- —, M.-S. Ahn, I.-S. Kang, and A. D. Del Genio, 2015: Role of longwave cloud–radiation feedback in the simulation of the Madden–Julian oscillation. *J. Climate*, 28, 6979–6994, https:// doi.org/10.1175/JCLI-D-14-00767.1.
- ——, H. Kim, and M. I. Lee, 2017: Why does the MJO detour the Maritime Continent during austral summer? *Geophys. Res. Lett.*, 44, 2579–2587, https://doi.org/10.1002/2017GL072643.
- —, E. D. Maloney, and C. Zhang, 2020: Review: MJO propagation over the Maritime Continent. *The Multiscale Global Monsoon System*, C. P. Chang et al., Eds., World Scientific Series on Asia-Pacific Weather and Climate, Vol. 11, 4th ed. World Scientific, 261–272, https://doi.org/10.1142/11723.
- Kim, H., F. Vitart, and D. E. Waliser, 2018: Prediction of the Madden–Julian oscillation: A review. J. Climate, 31, 9425– 9443, https://doi.org/10.1175/JCLI-D-18-0210.1.
- Kim, K. Y., K. Kullgren, G. H. Lim, K. O. Boo, and B. M. Kim, 2006: Physical mechanisms of the Australian summer

- monsoon: 2. Variability of strength and onset and termination times. *J. Geophys. Res.*, **111**, D20105, https://doi.org/10.1029/2005JD006808.
- Knutson, T. R., K. M. Weickmann, and J. E. Kutzbach, 1986: Global-scale intraseasonal oscillations of outgoing longwave radiation and 250 mb zonal wind during Northern Hemisphere summer. *Mon. Wea. Rev.*, 114, 605–623, https://doi. org/10.1175/1520-0493(1986)114<0605:GSIOOO>2.0.CO;2.
- Lee, Y.-Y., and G.-H. Lim, 2012: Dependency of the North Pacific winter storm tracks on the zonal distribution of MJO convection. J. Geophys. Res., 117, D14101, https://doi.org/10.1029/ 2011JD016417.
- Li, K., W. Yu, Y. Yang, L. Feng, S. Liu, and L. Li, 2020: Spring barrier to the MJO eastward propagation. Geophys. Res. Lett., 47, e2020GL087788, https://doi.org/10. 1029/2020GL087788.
- Liebmann, B., H. H. Hendon, and J. D. Glick, 1994: The Relationship between tropical cyclones of the western Pacific and Indian Oceans and the Madden–Julian oscillation. *J. Meteor. Soc. Japan*, **72**, 401–412, https://doi.org/10.2151/jmsj1965.72.3_401.
- Lin, H., G. Brunet, and J. Derome, 2009: An observed connection between the North Atlantic oscillation and the Madden– Julian oscillation. *J. Climate*, 22, 364–380, https://doi.org/10. 1175/2008JCLI2515.1.
- Lin, J.-L., and B. E. Mapes, 2004: Radiation budget of the tropical intraseasonal oscillation. *J. Atmos. Sci.*, **61**, 2050–2062, https://doi.org/10.1175/1520-0469(2004)061<2050: RBOTTI>2.0.CO;2.
- Lin, J. W. B., J. D. Neelin, and N. Zeng, 2000: Maintenance of tropical intraseasonal variability: Impact of evaporationwind feedback and midlatitude storms. *J. Atmos. Sci.*, 57, 2793–2823, https://doi.org/10.1175/1520-0469(2000)057<2793: MOTIVI>2.0.CO;2.
- Ling, J., C. Zhang, S. Wang, and C. Li, 2017: A new interpretation of the ability of global models to simulate the MJO. Geophys. Res. Lett., 44, 5798–5806, https://doi.org/10.1002/2017GL073891.
- Lisonbee, J., and J. Ribbe, 2021: Seasonal climate influences on the timing of the Australian monsoon onset. *Wea. Climate Dyn.*, **2**, 489–506, https://doi.org/10.5194/wcd-2-489-2021.
- Madden, R. A., and P. R. Julian, 1971: Detection of a 40–50 day oscillation in the zonal wind in the tropical Pacific. *J. Atmos. Sci.*, **28**, 702–708, https://doi.org/10.1175/1520-0469(1971)028
- —, and —, 1972: Description of global-scale circulation cells in the tropics with a 40–50 day period. *J. Atmos. Sci.*, **29**, 1109–1123, https://doi.org/10.1175/1520-0469(1972)029<1109: DOGSCC>2.0.CO;2.
- Maloney, E. D., and D. L. Hartmann, 2000: Modulation of eastern North Pacific hurricanes by the Madden–Julian oscillation. *J. Climate*, **13**, 1451–1460, https://doi.org/10.1175/1520-0442(2000) 013<1451:MOENPH>2.0.CO;2.
- —, and A. H. Sobel, 2004: Surface fluxes and ocean coupling in the tropical intraseasonal oscillation. *J. Climate*, **17**, 4368–4386, https://doi.org/10.1175/JCLI-3212.1.
- —, Á. F. Adames, and H. X. Bui, 2019: Madden–Julian oscillation changes under anthropogenic warming. *Nat. Climate Change*, 9, 26–33, https://doi.org/10.1038/s41558-018-0331-6.
- Matsuno, T., 1966: Quasi-geostrophic motions in the equatorial area. *J. Meteor. Soc. Japan*, **44**, 25–43, https://doi.org/10.2151/jmsj1965.44.1_25.

- Matthews, A. J., B. J. Hoskins, and M. Masutani, 2004: The global response to tropical heating in the Madden–Julian oscillation during the northern winter. *Quart. J. Roy. Meteor. Soc.*, 130, 1991–2011, https://doi.org/10.1256/qj.02.123.
- Meehl, G. A., and Coauthors, 2021: Initialized Earth system prediction from subseasonal to decadal timescales. *Nat. Rev. Earth Environ.*, 2, 340–357, https://doi.org/10.1038/s43017-021-00155-x.
- Narsey, S. Y., J. R. Brown, R. A. Colman, F. Delage, S. B. Power, A. F. Moise, and H. Zhang, 2020: Climate change projections for the Australian monsoon from CMIP6 models. *Geophys. Res. Lett.*, 47, e2019GL086816, https://doi.org/10.1029/2019GL086816.
- Rayner, N. A., D. E. Parker, E. B. Horton, C. K. Folland, L. V. Alexander, D. P. Rowell, E. C. Kent, and A. Kaplan, 2003: Global analyses of sea surface temperature, sea ice, and night marine air temperature since the late nine-teenth century. J. Geophys. Res., 108, 4407, https://doi.org/10.1029/2002JD002670.
- Rushley, S. S., D. Kim, C. S. Bretherton, and M. S. Ahn, 2018: Reexamining the nonlinear moisture-precipitation relationship over the tropical oceans. *Geophys. Res. Lett.*, 45, 1133–1140, https://doi.org/10.1002/2017GL076296.
- —, and Á. F. Adames, 2019: Changes in the MJO under greenhouse gas-induced warming in CMIP5 models. *J. Climate*, **32**, 803–821, https://doi.org/10.1175/JCLI-D-18-0437.1.
- Seo, K.-H., and S.-W. Son, 2012: The Global atmospheric circulation response to tropical diabatic heating associated with the Madden–Julian oscillation during northern winter. *J. Atmos. Sci.*, 69, 79–96, https://doi.org/10.1175/2011JAS3686.1.
- Shi, X., D. Kim, Á. F. Adames, and J. Sukhatme, 2018: WISHE-moisture mode in an aquaplanet simulation. J. Adv. Model. Earth Syst., 10, 2393–2407, https://doi.org/10. 1029/2018MS001441.
- Singh, B., and J. L. Kinter, 2020: Tracking of tropical intraseasonal convective anomalies: 1. Seasonality of the tropical intraseasonal oscillations. *J. Geophys. Res. Atmos.*, 125, e2019JD030873, https://doi.org/10.1029/2019JD030873.
- Sobel, A., and E. Maloney, 2012: An idealized semi-empirical framework for modeling the Madden–Julian oscillation. J. Atmos. Sci., 69, 1691–1705, https://doi.org/10.1175/JAS-D-11-0118.1.
- —, and —, 2013: Moisture modes and the eastward propagation of the MJO. *J. Atmos. Sci.*, **70**, 187–192, https://doi.org/10.1175/JAS-D-12-0189.1.
- ——, G. Bellon, and D. M. Frierson, 2008: The role of surface heat fluxes in tropical intraseasonal oscillations. *Nat. Geosci.*, **1**, 653–657, https://doi.org/10.1038/ngeo312.
- —, —, and —, 2010: Surface fluxes and tropical intraseasonal variability: A reassessment. *J. Adv. Model. Earth Syst.*, **2**, 2, https://doi.org/10.3894/JAMES.2010.2.2.
- Takayabu, Y. N., T. Iguchi, M. Kachi, A. Shibata, and H. Kanzawa, 1999: Abrupt termination of the 1997–98 El Niño in response to a Madden–Julian oscillation. *Nature*, 402, 279–282, https://doi.org/10.1038/46254.
- Tseng, K. C., E. Maloney, and E. Barnes, 2019: The consistency of MJO teleconnection patterns: An explanation using linear Rossby wave theory. *J. Climate*, 32, 531–548, https://doi.org/ 10.1175/JCLI-D-18-0211.1.
- Wang, B., and H. Rui, 1990: Synoptic climatology of transient tropical intraseasonal convection anomalies: 1975–1985. *Meteor. Atmos. Phys.*, 44, 43–61, https://doi.org/10.1007/ BF01026810.

- —, G. Chen, and F. Liu, 2019: Diversity of the Madden-Julian oscillation. Sci. Adv., 5, eaax022, https://doi.org/10.1126/sciadv.aax0220.
- Wheeler, M. C., and H. H. Hendon, 2004: An all-season real-time multivariate MJO index: Development of an index for monitoring and prediction. *Mon. Wea. Rev.*, 132, 1917–1932, https://doi.org/10.1175/1520-0493(2004)132<1917: AARMMI>2.0.CO;2.
- —, and J. L. McBride, 2005: Australian-Indonesian monsoon. Intraseasonal Variability in the Atmosphere-Ocean Climate System, M. C. Wheeler and J. L. McBride, Eds., Vol. 5, Springer Praxis Books, 125–174.
- Wu, C. H., and H. H. Hsu, 2009: Topographic influence on the MJO in the Maritime Continent. J. Climate, 22, 5433–5448, https://doi.org/10.1175/2009JCLI2825.1.

- Yasunari, T., 1979: Cloudiness fluctuations associated with the Northern Hemisphere summer monsoon. *J. Meteor. Soc. Japan*, **57**, 227–242, https://doi.org/10.2151/jmsj1965. 57.3 227.
- Zhang, C., and M. Dong, 2004: Seasonality in the Madden–Julian oscillation. *J. Climate*, **17**, 3169–3180, https://doi.org/10.1175/1520-0442(2004)017<3169:SITMO>2.0.CO;2.
- —, and J. Ling, 2017: Barrier effect of the Indo-Pacific Maritime Continent on the MJO: Perspectives from tracking MJO precipitation. *J. Climate*, **30**, 3439–3459, https://doi.org/10.1175/JCLI-D-16-0614.1.
- Zhou, L., and R. Murtugudde, 2020: Oceanic impacts on MJOs detouring near the Maritime Continent. *J. Climate*, **33**, 2371–2388, https://doi.org/10.1175/JCLI-D-19-0505.1.